

Supporting Information

Confining Sb_2Se_3 nanorod yolk in mesoporous carbon shell with an in-built buffer space for stable Li-ion batteries

Yingmeng Zhang¹, Shaojun Li¹, Lele Cheng¹, Yongliang Li¹, Xiangzhong Ren¹,
Peixin Zhang¹, Lingna Sun^{1*}, and Hui Ying Yang^{2*}

¹College of Chemistry and Environmental Engineering, Shenzhen University,
Shenzhen, Guangdong 518060, P.R. China

²Pillar of Engineering Product Development, Singapore University of Technology and
Design, 8 Somapah Road, 487372, Singapore.

Corresponding author:

Lingna Sun, Email: sunln@szu.edu.cn, Tel: +86-755-26538657

Hui Ying Yang, E-mail: yanghuiying@sutd.edu.sg

Experimental

Material Synthesis

All the materials and chemicals used in this study were of analytical grade and directly used as received from the Aladdin manufacturers.

Synthesis of Sb₂Se₃ nanorods.

Sb₂Se₃ nanorods were synthesized through a facile solvothermal method. Typically, 2 mmol of SbCl₃ was added into 60 mL of poly (ethylene glycol)-200 (PEG-200) and stirred for 2 h. Separately, the hydrazine hydrate-Se solution prepared by mixing 4 mmol of Se and 10 mL of hydrazine hydrate (N₂H₄•H₂O, 80wt%). The solution was added dropwise into the above organic mixture and continuously stirred for 4 h. Then, the mixed solution was transferred into a 100 mL Teflon-lined stainless-steel autoclave, sealed and maintained at 200 °C for 12 h. Finally, after cooling down to room temperature, the as-prepared product of Sb₂Se₃ nanorods, were collected by centrifugation and washed with deionized water and ethanol for three times before vacuum drying overnight at 60 °C.

Synthesis of Sb₂Se₃@SiO₂ core-shell nanorods

In a typical synthesis, 0.25 g of Sb₂Se₃ nanorods were dispersed into a mixture of isopropanol (97 mL), deionized water (9 mL), and ammonia (5 mL, 25wt%) by sonication. After ultrasonic dispersion for 10 min, 0.1 mL tetraethyl orthosilicate (TEOS) was added to the above solution. Then the dispersion was further stirred for 2 h at 40 °C. Afterwards, the core-shell Sb₂Se₃@SiO₂ nanorods were obtained after centrifugation and washing with ethanol several times.

Synthesis of Sb₂Se₃@Void@C yolk-shell nanorods

The 0.2 g of as-prepared Sb₂Se₃@SiO₂ nanorods and 0.115 g of cetyltrimethylammonium bromide (CTAB) were added into a mixture with 7 mL of deionized water and 14 mL of alcohol. After 0.5 h ultra-sonication and 0.5 h stirring, 0.0175 g of resorcinol and 0.05 mL of ammonia (25wt%) were added sequentially. The mixture in the beaker was stirred for an additional 0.5 h at room temperature and then 0.06 mL of formaldehyde was finally added. The above mixture was continually stirred for 12 h, the precipitates were obtained and washed with water and ethanol several times, and dried at 60 °C overnight. Sb₂Se₃@Void@C yolk-shell nanorods were obtained after carbonization at 500 °C under argon for 3 h and removal of silica by 8wt% hydrofluoric acid

(HF) solution for 12 h.

Synthesis of Sb₂Se₃@C core-shell nanorods

The Sb₂Se₃@C core-shell nanorods were also prepared for comparison in electrochemical performance. Similarly, 0.2 g of Sb₂Se₃ nanorods were directly reacted with resorcinol and formaldehyde, instead of SiO₂ pre-coating and afterwards HF etching.

Material characterization

Field-emission scanning electron microscopy (FE-SEM, JSM-7800F & TEAM Octane Plus, 10 kV, Japan) was used to characterize the morphology and size of the obtained samples. Transmission electron microscopy (TEM, JEM-2100 and X-Max 80, 200-300 kV, Japan) was performed to observe the internal structure of the sample, the lattice parameters and the elements. X-ray diffraction was performed on a PANalytical X'pert PRO X-ray diffractometer (XRD, PANalytical Empyrean, Netherlands) with a Cu-K α radiation at 45 kV and 40 mA. The chemical states and elements in the samples were identified by X-ray photoelectron spectroscopy (XPS, Thermo Scientific K-Alpha⁺, UK). Thermogravimetric analysis (TGA, Q50, Germany) was performed in a temperature range of 30-800 °C with a heating rate of 10 °C min⁻¹ in air. Raman spectroscopy (Renishaw inVia) is a technique to detect the confusion and defect degree of material. Specific surface area and pore size distributions were obtained by using the Brunauer-Emmett-Teller method (BET, NOVA1200e).

Electrochemical measurements

The active electrode material, acetylene black and carboxymethyl cellulose (CMC) were mixed in deionized water with a weight ratio of 8:1:1, which was coated directly on Cu foil and dried at 60 °C under vacuum overnight. The prepared electrode was cut into discs with diameter of 14 mm, and the typical mass loading is about 1.0 mg cm⁻². The electrochemical performance was investigated by using CR2032 coin-type cell. The metallic lithium foil and Celgard polymer membrane were used as the counter electrode and separator, respectively. The electrolyte was 1 M LiPF₆ in EC/DMC/EMC (1:1:1 by volume ratio). The charge-discharge tests were performed at a potential range of 0.01-3.0 V using a LAND CT2001A instrument (Wuhan, China). Cyclic voltammetry (CV) was measured at a scan rate of 0.2 mV s⁻¹ between 0.01 and 3 V using an electrochemical station (CHI760E, China). The electrochemical impedance spectroscopy (EIS) was collected by CHI760E electrochemical station in the frequency range of 100 kHz to 0.01 Hz,

which was obtained at an AC potential amplitude of 5 mV around the open circuit before the electrochemical performance testing. The mass loading of the $\text{Sb}_2\text{Se}_3@\text{Void}@C$ yolk-shell nanorods was calculated based on the total mass of the composite including the carbon shell.

In situ XRD measurements

In situ XRD measurements were performed in the Swagelok-type cell at current density of 100 mA g^{-1} within a potential window from 0.01 to 3.0 V. The active electrode material mixed with acetylene black and CMC in a weight ratio of 8:1:1, was coated directly on Beryllium (Be) foil and dried at $60 \text{ }^\circ\text{C}$ under vacuum overnight. The electrode was assembled in the glove-box with a Swagelok-type cell, which was connected to the LAND CT2001A battery testing system during the in situ XRD measurements.

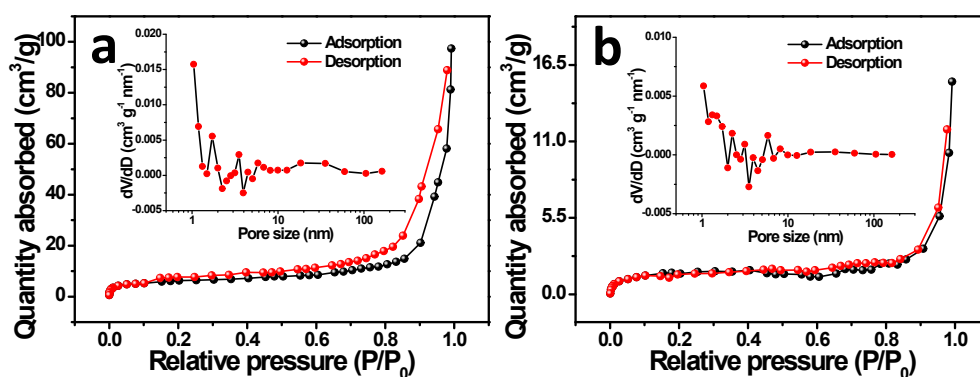


Figure S1. N₂ adsorption/desorption isotherms and the corresponding pore size distribution of (a) Sb₂Se₃@Void@C and (b) Sb₂Se₃.

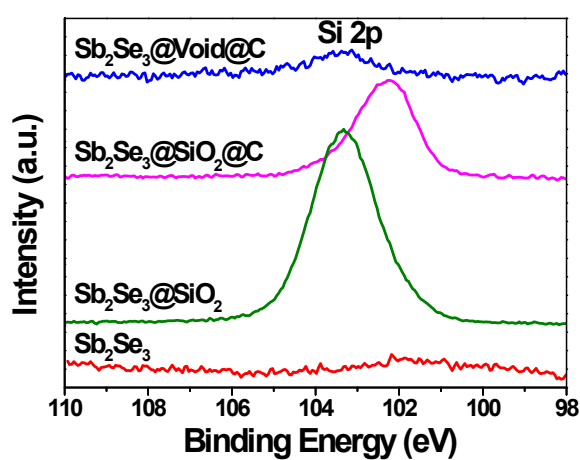


Figure S2. Si 2p core level XPS spectra of the pristine Sb₂Se₃, precursor Sb₂Se₃@SiO₂, intermediate Sb₂Se₃@SiO₂@C and final Sb₂Se₃@Void@C composite samples.

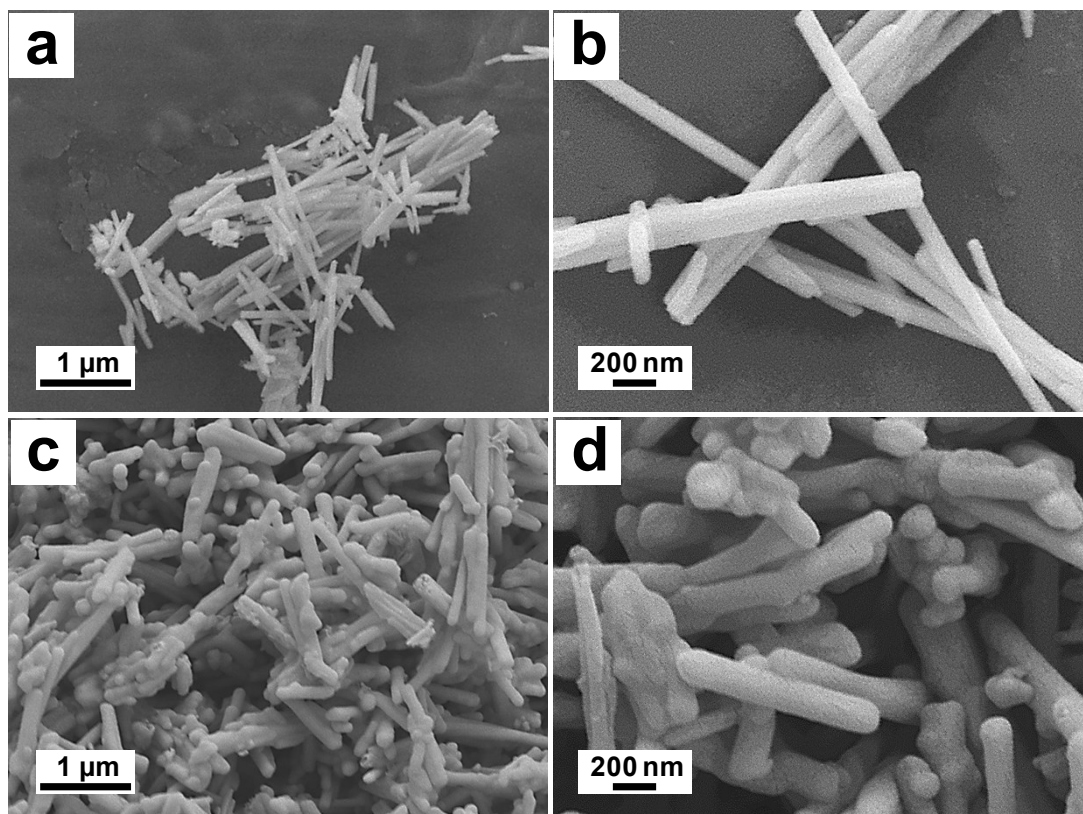


Figure S3. FESEM images of the obtained samples: (a, b) precursor $\text{Sb}_2\text{Se}_3@\text{SiO}_2$ and (c, d) intermediate $\text{Sb}_2\text{Se}_3@\text{SiO}_2@\text{C}$.

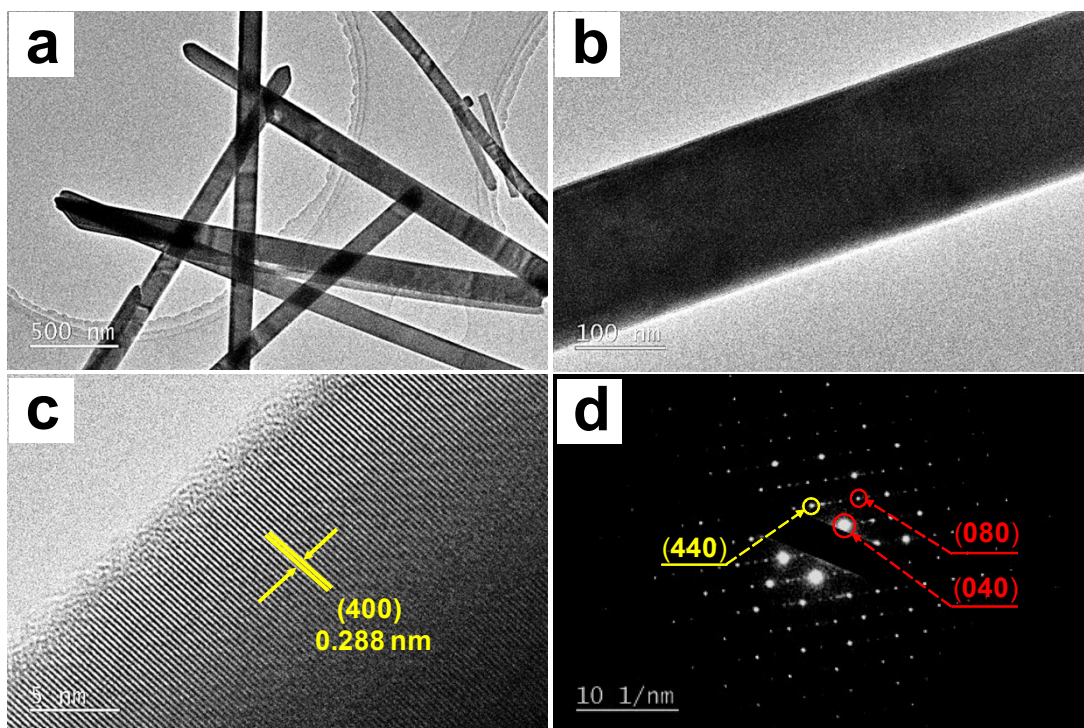


Figure S4. (a, b) TEM images and (c) HRTEM image for the Sb_2Se_3 sample; (d) the corresponding selected area electron diffraction (SAED) pattern.

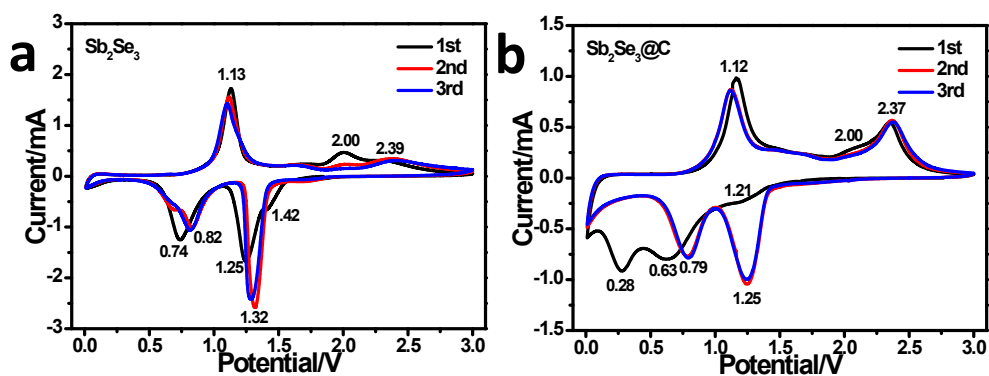


Figure S5. CV curves for the first 3 cycles at a scan rate of 0.2 mV s^{-1} in the voltage range of 0.01-3.0 V for the pristine Sb_2Se_3 (a) and comparative $\text{Sb}_2\text{Se}_3@\text{C}$ (b) samples.

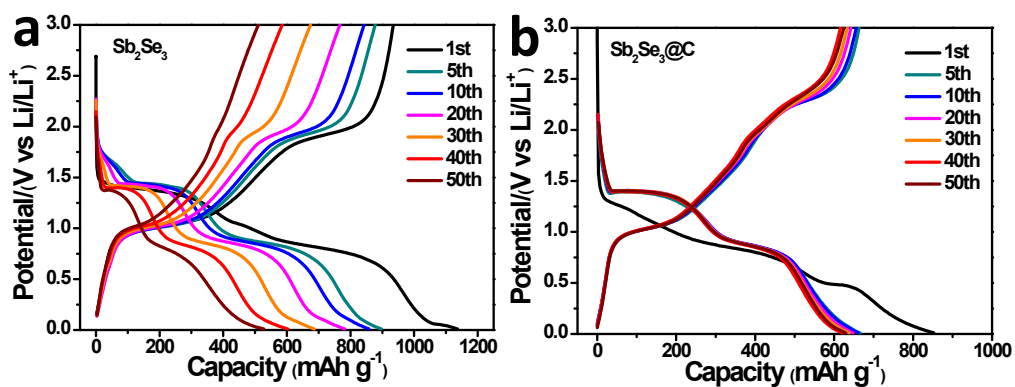


Figure S6. Charge/discharge profiles at a current density of 0.2 A g^{-1} for the pristine Sb_2Se_3 (a) and comparative $\text{Sb}_2\text{Se}_3@\text{C}$ (b) samples.

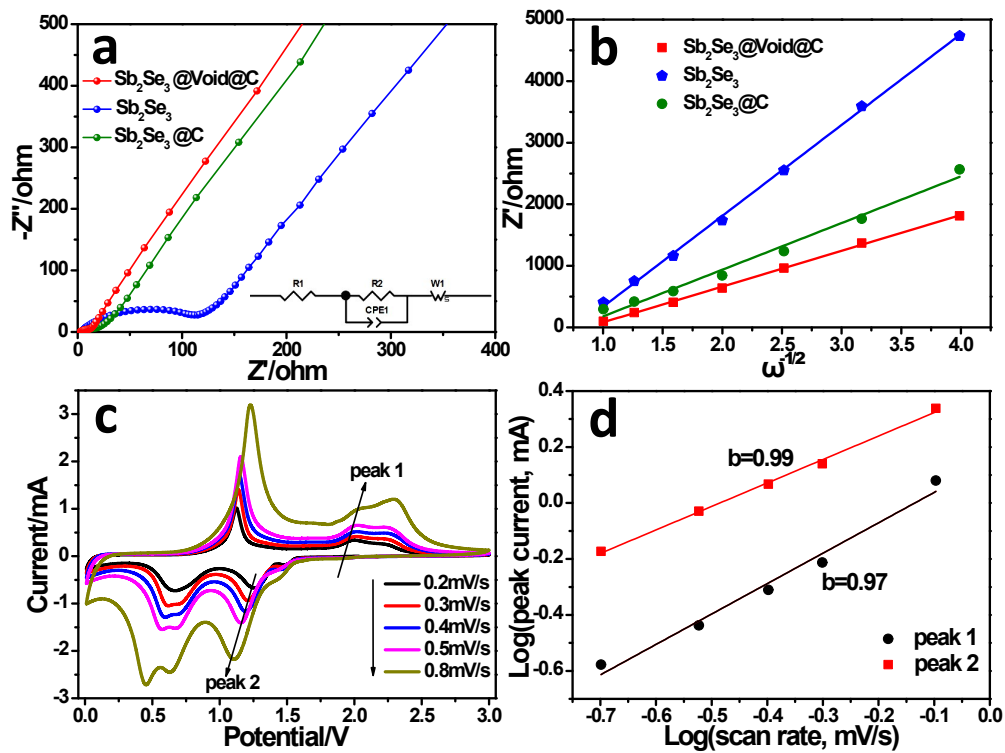


Figure S7. (a) Nyquist plots and (b) Z' vs $\omega^{-1/2}$ in the low-frequency regions of $\text{Sb}_2\text{Se}_3@Void@C$, Sb_2Se_3 and $\text{Sb}_2\text{Se}_3@C$; (c) CV curves at different scan rates and (d) plots for $\log(i)$ versus $\log(v)$ (peak current, i ; scanning rate, v) for $\text{Sb}_2\text{Se}_3@Void@C$.

Table S1. Comparison of the performance between yolk-shell Sb_2Se_3 nanorods with other reported Sb_2Se_3 studies as anode materials for LIBs

Samples	Cycling		Cycling		Rate	Rate	Ref.
	current (A g^{-1})	Cycles	capacity (mA h g^{-1})	current (A g^{-1})	capacity (mA h g^{-1})		
$\text{Sb}_2\text{Se}_3@\text{Void}@C$	0.2	100	658.6	2.0	625.3	This	work
				3.0	594.7		
$\text{Sb}_2\text{Se}_3/\text{rGO}$	0.1	100	430	1.0	247	[1]	
Sb_2Se_3 nanowires	0.1	50	650.2	2.0	389.5	[2]	
Amorphous $\text{Sb}_2\text{Se}_3/C$	0.1	100	662	1.95	623	[3]	
Sb_2Se_3 nanowire membrane	0.1	50	584	1.6	255	[4]	
Sb_2Se_3 nanorods	0.067	100	230	0.67	120	[5]	
$\text{Ge}_2\text{Sb}_2\text{Se}_5$ glass	0.424	100	626	0.848	554	[6]	
$\text{Sb}_2\text{Se}_3@\text{C}$ nanofibers	0.1	100	625	2.0	400	[7]	

Table S2. R_2 , σ and D_{Li^+} values for the $\text{Sb}_2\text{Se}_3@\text{Void}@C$, Sb_2Se_3 and $\text{Sb}_2\text{Se}_3@\text{C}$ electrodes

	R_2 (Ω)	σ ($\Omega \text{ cm}^2\text{s}^{-0.5}$)	D_{Li^+} (cm^2s^{-1})
$\text{Sb}_2\text{Se}_3@\text{Void}@C$	16	580.8	4.8×10^{-16}
Sb_2Se_3	134.4	1476.4	7.6×10^{-17}
$\text{Sb}_2\text{Se}_3@\text{C}$	29	758.1	2.8×10^{-16}

References:

1. Y. Tian, Z. Sun, Y. Zhao, Y. Zhang, T. Tan, F. Yin, *Journal of Nanoparticle Research* **2019**, 21, 15.
2. W. Luo, J.-J. Gaumet, P. Magri, S. Diliberto, F. Li, P. Franchetti, J. Ghanbaja, L. Mai, *Journal of Energy Chemistry* **2019**, 30, 27.
3. K.-H. Nam, C.-M. Park, *Journal of Power Sources* **2019**, 433, 126639.
4. W. Luo, A. Calas, C. Tang, F. Li, L. Zhou, L. Mai, *ACS Appl Mater Interfaces* **2016**, 8, 35219.
5. Y. Tian, Z. Sun, Y. Zhao, T. Tan, H. Liu, Z. Chen, *Journal of Nanomaterials* **2018**, 2018, 1.
6. J. R. Rodriguez, Z. M. Qi, H. Y. Wang, M. Y. Shalaginov, C. Goncalves, M. Karig, K. A. Richardson, J. Guerrero-Sanchez, M. G. Moreno-Armenta, V. G. Pol, *Nano Energy* **2020**, 68, 104326.
7. Y. Dong, Y. Z. Feng, J. W. Deng, P. B. He, J. M. Ma, *Chinese Chem Lett* **2020**, 31, 909.